Colloquium: New physics search with flavor in the LHC era

Tobias Hurth*

PRISMA Cluster of Excellence and Institute for Physics (THEP), Johannes Gutenberg University, D-55099 Mainz, Germany

Farvah Mahmoudi†

CERN Theory Division, Physics Department, CH-1211 Geneva 23, Switzerland and Clermont Université, Université Blaise Pascal, CNRS/IN2P3, LPC, BP 10448, 63000 Clermont-Ferrand, France

(published 15 May 2013)

A status report on quark flavor physics in view of the latest data from the B factories and the LHC is given, and the impact of the latest experimental results on new physics in the minimal flavor violation framework is discussed. Also shown are some examples of the implications in supersymmetry.

DOI: 10.1103/RevModPhys.85.795 PACS numbers: 13.20.He, 12.15.Ff, 12.15.Hh

CONTENTS

I. STANDARD MODEL AND NEW PHYSICS FLAVOR PROBLEMS

At the end of the B factories at SLAC (*BABAR* experiment) (BABAR Collaboration) and at KEK (Belle experiment) (Belle Collaboration) and of the Tevatron B physics experiments (CDF Collaboration; D0 Collaboration), all present measurements in flavor physics are consistent with the simple Cabibbo-Kobayashi-Maskawa (CKM) theory of the standard model (SM). The recent measurements by the high-statistics LHCb experiment (LHCb Collaboration) have not changed this feature. Of course there have been and there are still so-called tensions, anomalies, or puzzles in the quark flavor data at the 1σ, 2σ, or 3σ level, however, until now they all have disappeared after some time when more statistics have been collected.

Thus, at least at present all flavor-violating processes between quarks are well described by a 3×3 unitarity matrix, usually referred to as the CKM matrix (Cabibbo, 1963; Kobayashi and Maskawa, 1973), which is fully described by four real parameters, three rotation angles, and one complex phase. It is this complex phase that represents the only source of CP violation in the SM and that allows for a unified description of all the CP violating phenomena. This is an impressing success of the SM and the CKM theory.

It is illustrated by the overconstrained triangles in the complex plane which reflect the unitarity of the CKM matrix; see Fig. 1. Some historical CKM fits in Fig. 2 illustrate the great success of the B factories. A closer look at the constraints is even more impressive: the constraints induced by CP conserving and by CP violating observables are fully consistent with each other (see Fig. 3). Moreover, the tree-level observables which are in general assumed not being affected by new physics effects provide constraints which are fully consistent with the ones obtained from loop-induced observables (see Fig. 4). Especially this feature is somehow unexpected because in principle (loop-induced) flavor-changing neutral current (FCNC) processes like $\bar{B} \to X_s \gamma$ offer high sensitivity to new physics (NP) due to the simple fact that additional contributions to the decay rate, in which SM particles are replaced by new particles such as the supersymmetric charginos or gluinos, are not suppressed by the loop factor $\alpha/4\pi$ relative to the SM contribution; see Fig. 5.

It is worth mentioning that there is much more flavor data not shown in the unitarity fits which confirms the SM

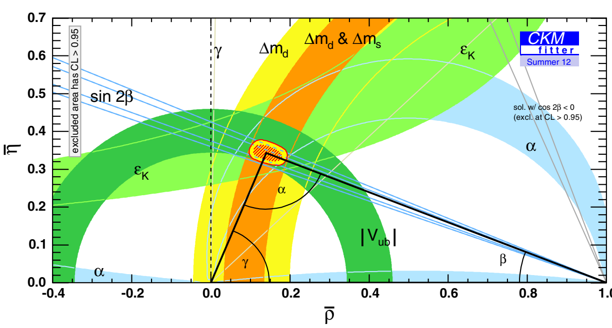

FIG. 1 (color online). Constraints in the $(\bar{\rho}, \bar{\eta})$ plane. The hashed region of the global combination corresponds to 68% C.L. From Charles *et al.*, 2005.

*tobias.hurth@cern.ch
†mahmoudi@in2p3.fr

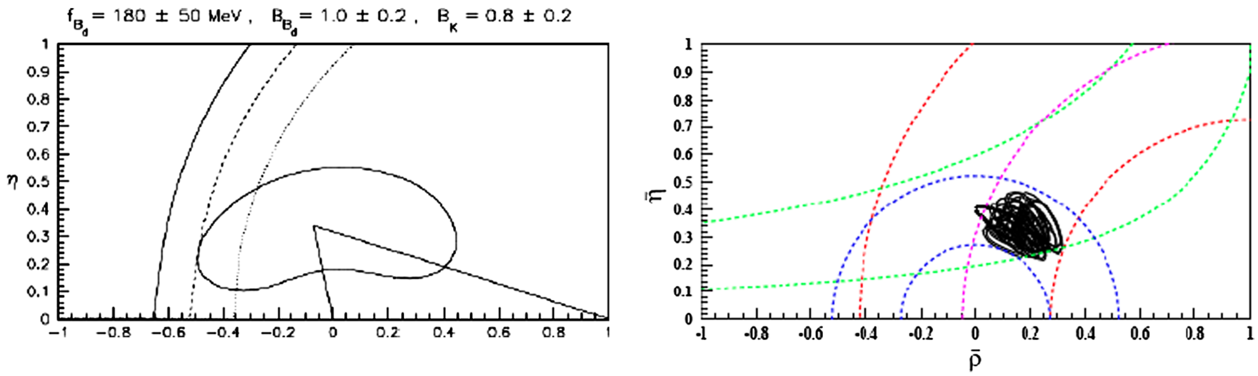

FIG. 2 (color online). Historical CKM fits of Ali and London (1995)) (left) and of Plazczynski and Schune (BABAR Collaboration, 1998) (right).

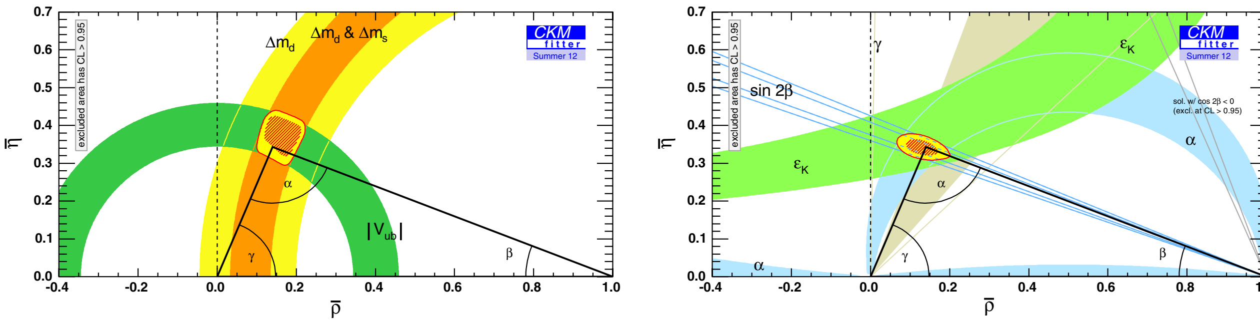

FIG. 3 (color online). Constraints from *CP* conserving (left) and *CP* violating (right) quantities only. From Charles *et al.*, 2005.

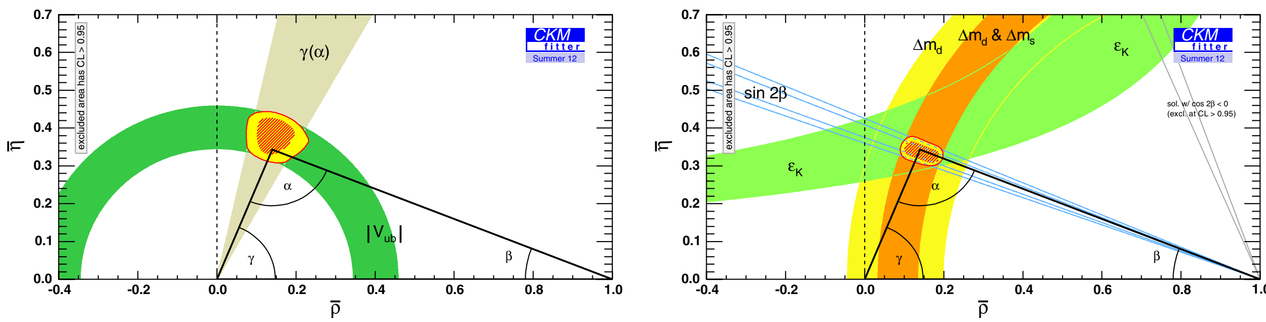

FIG. 4 (color online). Constraints from "tree" (left) and "loop" (right) quantities only. From Charles *et al.*, 2005.

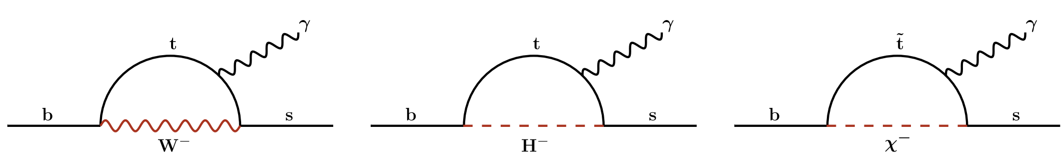

FIG. 5 (color online). Loop-induced $\bar{B} \to X_s \gamma$ decay via the SM particles, W^- boson, and top quark t (left), via new particle, namely, charged Higgs H^- and top quark t (middle), or via new supersymmetric particles, chargino $\tilde{\chi}^-$, and stop $\tilde{t}$ (right).

predictions of flavor mixing like rare decays. The success of the CKM theory was honored by the Nobel Prize in physics in 2008.

The absence of any unambiguous sign for NP in the flavor data but also in the high-p_T data of the ATLAS and CMS experiments (ATLAS Collaboration; CMS Collaboration) guides our attention to the well-known flavor problem of NP: in the model-independent approach using the effective electroweak Hamiltonian, the contribution to one six-dimensional specific operator $\mathcal{O}_i$ can be parametrized via $[C^i_{\rm SM}/(M_W)^2 + C^i_{\rm NP}/(\Lambda_{\rm NP})^2] \times \mathcal{O}_i$, where the first term represents the SM contribution at the electroweak scale M_W and the second one the NP contribution with an unknown coupling $C^i_{\rm NP}$ and an unknown NP scale $\Lambda_{\rm NP}$. The nonexistence of large NP effects in FCNC observables in general asks for an explanation why FCNCs are suppressed. This famous flavor problem of NP can be solved in two ways: either the mass scale of the new degrees of freedom $\Lambda_{\rm NP}$ is very high or the new flavor-violating couplings $C^i_{\rm NP}$ are small for (symmetry?) reasons that remain to be found. For example, assuming *generic* new flavor-violating couplings of $O(1)$, the present data on K-$\bar{K}$ mixing implies a very high NP scale of the order of 10^3–10^4 TeV depending on whether the new contributions enter at loop or at tree level. In contrast, theoretical considerations on scale hierarchies in the Higgs sector, which is responsible for the mass generation of the fundamental particles in the SM, call for NP at the order of 1 TeV. But any NP below the 1 TeV scale must have a nongeneric flavor structure.

These considerations also imply that FCNC decays provide information about the SM and its extensions via virtual effects to scales presently not accessible by the direct search for new particles [for reviews see Hurth (2003) and Hurth and Nakao (2010)]. Thus, the information offered by the FCNC is complementary to the one provided by the high-p_T experiments ATLAS and CMS (Hurth and Kraml, 2012; Mahmoudi, 2012). It is also obvious that the indirect information on NP by FCNC (even if SM like) is most valuable when the general nature of NP is identified in the direct search, especially when the mass scale of NP is fixed.

Indeed, in the SM the Glashow-Iliopoulos-Maiani (GIM) mechanism, small CKM elements, and often helicity all suppress FCNC processes. These suppression factors stem from the particle content of the SM and the unexplained smallness of most Yukawa couplings and are absent in generic extensions of the SM. Hence FCNCs are an excellent testing ground to probe new physics up to scales of 100 TeV, depending on the model. Moreover, CP violation in flavor-changing transitions of the SM is governed by a single parameter, the phase of the CKM matrix, so that the SM is highly predictive about CP physics. Certain CP asymmetries are practically free of hadronic uncertainties, which permits the extraction of fundamental CP phases from experiments with high accuracy. Thus, CP physics is a powerful tool to probe extensions of the SM, which generically involve many new CP phases.

As a consequence, the present data of the B physics experiments already imply significant restrictions for the parameter space of new physics models(as we explicitly show) and lead to important clues for the direct search for new particles and for model building beyond the SM.

Thus, the CKM mechanism is the dominating effect for CP violation and flavor mixing in the quark sector; however, there is still room for sizable new effects and new flavor structures because the flavor sector has been tested only at the 10% level especially in the b-s sector. Moreover, the standard model does not describe the flavor phenomena in the lepton sector due to the existence of neutrino masses, a property not described by the SM. Furthermore, while the gauge principle governs the gauge sector of the SM there is no guiding principle in the flavor sector: the CKM mechanism (three Yukawa SM couplings) provides a phenomenological description of quark flavor processes, but leaves the significant hierarchy of the quark masses and the mixing parameters—observed in experiment—unexplained. This problem is often referred to as the flavor problem of the SM.

There are many solutions to this problem proposed in the literature, for example, the Froggatt-Nielsen mechanism (Froggatt and Nielsen, 1979) and the Nelson-Strassler mechanism (Nelson and Strassler, 2000); the popular Randall-Sundrum model is another approach to this SM flavor problem, where the hierarchy of the flavor parameters can be explained by the special geometrical settings of the model. In addition the so-called gauge-hierarchy problem in the Higgs sector finds a natural explanation in this model (Randall and Sundrum, 1999; Gherghetta and Pomarol, 2000; Grossman and Neubert, 2000).

The SM flavor problem is also reflected in the fact that many open fundamental questions of particle physics are related to flavor:

- How many families of fundamental fermions are there?
- How are neutrino and quark masses and mixing angles generated?
- Do new sources of flavor and CP violation exist?
- Is there CP violation in the QCD gauge sector?
- Are there relations between the flavor structure in the lepton and quark sectors?

There is already experimental evidence beyond the SM which is partially connected to flavor physics: the existence of dark matter, the nonzero neutrino masses, and the baryon asymmetry of the Universe; the latter implies the need for new sources of CP violation beyond the one offered by the SM. This provides an important link between particle physics and cosmology.

In the following sections, we discuss the latest key measurements by LHCb, the B factories, and the Tevatron experiments.

II. LATEST MEASUREMENTS AT HADRON COLLIDERS

A. New physics in B_q-$\bar{B}_q$ mixing ($q = d, s$)?

The meson-antimeson oscillation is governed by two parameters, the mass difference (ΔM) of the two physical eigenstates B_H and B_L and the decay rate difference ($\Delta\Gamma$):

$$\Delta M := M_H - M_L = 2|M_{12}|, \quad (1)$$

$$\Delta\Gamma := \Gamma_L - \Gamma_H = 2|\Gamma_{12}|\cos\Phi. \quad (2)$$

$|M_{12}|$ corresponds to the dispersive part of the box diagram in Fig. 6 which is sensitive to new heavy particles, while Γ_{12} corresponds to its absorptive part which is sensitive to the light internal particles, and, thus, often assumed to be insensitive to NP. Possible NP effects can be parametrized by the complex parameter $\Delta_q (q = d, s)$: $M_{12,q} = M^{\rm SM}_{12,q} \times \Delta_q$ in a model-independent way. There are several observables which are sensitive to the NP phase $\arg(\Delta_q) = \Phi^\Delta_q$, for example, ΔM_q and $\Delta|\Gamma_q| = 2|\Gamma_{12,q}| \times \cos(\Phi^{\rm SM}_q + \Phi^\Delta_q)$. But also the golden modes $B_d \to J/\psi K^0_s$ and $B_s \to J/\psi\Phi$ are sensitive to

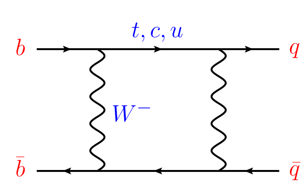

FIG. 6 (color online). B_q-$\bar{B}_q$ mixing governed by the box diagram.

the NP phases. The corresponding CP violating phases in the SM $\beta_q^{\rm SM}$ are modified via $2\beta_d^{\rm SM} + \Phi_d^\Delta$ and $2\beta_s^{\rm SM} - \Phi_s^\Delta$.

As illustrated in Fig. 7, the CP violating phase in $B_s \to J/\psi\Phi$ is very small in the SM (Lenz *et al.*, 2011):

$$2\beta_s^{\rm SM} = -\arg[(V_{ts}V_{tb}^*)^2/(V_{cs}V_{cb}^*)^2] = (2.1 \pm 0.1)°. \quad (3)$$

LHCb reported a measurement of this small angle (Aaij *et al.*, 2012b) which is fully consistent with the SM prediction and also consistent with the previous measurements of CDF and D0. In addition, LHCb resolved the twofold ambiguity (Aaij *et al.*, 2012a) and reported their first measurement of $\Delta\Gamma_s$ which confirms the heavy quark expansion prediction:

$$\Delta\Gamma_s(\text{LHCb}) = 0.116 \pm 0.019\ \text{ps}^{-1} \quad (4)$$

(Aaij *et al.*, 2012a, 2012b),

$$\Delta\Gamma_s(\text{HFAG}) = 0.105 \pm 0.015\ \text{ps}^{-1} \quad (5)$$

(Amhis *et al.*, 2012),

$$\Delta\Gamma_s(\text{SM}) = 0.087 \pm 0.021\ \text{ps}^{-1} \quad (6)$$

(Lenz and Nierste, 2011), and

$$\phi_s(\text{LHCb}) = -0.001 \pm 0.104\ \text{rad} \quad (7)$$

(Aaij *et al.*, 2012a, 2012b),

$$\phi_s(\text{HFAG}) = (-0.044^{+0.090}_{-0.085})\ \text{rad} \quad (8)$$

(Amhis *et al.*, 2012),

$$\phi_s(\text{SM}) = (-0.036 \pm 0.002)\ \text{rad} \quad (9)$$

(Lenz and Nierste, 2011). Thus, NP contributions in the mixing of the B_s system are disfavored by the present data (see Fig. 8).

Furthermore, the semileptonic asymmetries offer an independent test of NP physics in B_q-$\bar{B}_q$ mixing. In the presence of NP they get modified via

$$a_{sl}^q = \text{Im}\left(\frac{\Gamma_{12,q}}{M_{12,q}}\right) = \left(\frac{|\Gamma_{12,q}|}{|M_{12,q}|}\right)\frac{\sin(\Phi_q^{\rm SM} + \Phi_q^\Delta)}{|\Delta_q|}. \quad (10)$$

D0 measured the dimuon charge asymmetry to disagree with the SM prediction by 3.9σ (Abazov *et al.*, 2011; Lenz and Nierste, 2011):

$$A_{sl}^b(\text{D0}) = -(7.87 \pm 1.72 \pm 0.93) \times 10^{-3}, \quad (11)$$

$$A_{sl}^b(\text{SM}) = -(0.28^{+0.05}_{-0.06}) \times 10^{-3}, \quad (12)$$

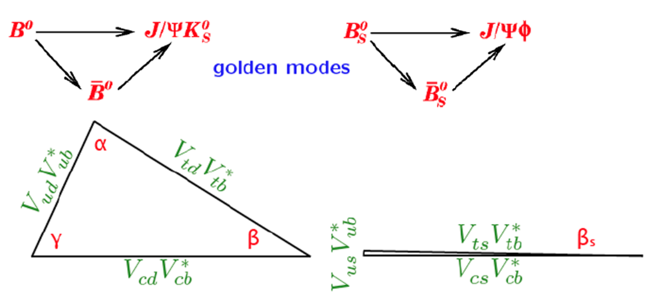

FIG. 7 (color online). CP violating through interference of decay with and without mixing in the two golden modes of the B_d and B_s system.

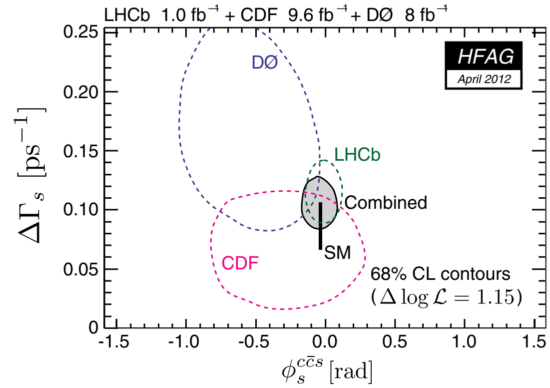

FIG. 8 (color online). HFAG 2012 combination of ϕ_s and $\Delta\Gamma_s$ results. From Amhis *et al.*, 2012.

where A_{sl}^b is a linear combination of the semileptonic asymmetries a_{sl}^d and a_{sl}^s. As argued by Lenz (2011), the central value of the D0 measurement is larger than theoretically possible. More recently, there are also direct measurements of a_{sl}^s and a_{sl}^d by D0 (Abazov *et al.*, 2013) which in combination with the dimuon charge asymmetry still lead to a 3σ deviation from the SM prediction; see the left plot of Fig. 9. In contrast, the first LHCb measurement of a_{sl}^s (LHCb Collaboration, 2012b) and the measurement of a_{sl}^d by the B factories (Amhis *et al.*, 2012) are compatible with the SM predictions; see the right plot of Fig. 9. Obviously, there is a slight tension between the two data sets which calls for improved measurements.

Finally, we mention that within the model-independent analysis of NP in B_d-$\bar{B}_d$ mixing, a 1.6σ deviation is obtained for the two-dimensional SM hypothesis $\Delta_d = 1$. Figure 10 shows the fit result for the complex parameter Δ_d. It is worth mentioning that a NP phase $\Phi_d^\Delta < 0$ would resolve the slight tension between $\text{BR}(B \to \tau\nu)$ and $\sin\beta$ in the global CKM fit (see Sec. III.B). We also state that in the B_s system the CKM fitter group finds a 0.2σ deviation for the corresponding SM hypothesis $\Delta_s = 1$; see Fig. 10. A detailed discussion can be found in Lenz *et al.* (2012).

B. Angular observables in $B \to K^*\ell^+\ell^-$

The semileptonic decay $B \to K^*\ell^+\ell^-$ is mediated by electroweak loop diagrams in the SM and can receive large enhancements from NP. It gives access to a variety of angular observables and hence offers a rich phenomenology. From a theoretical point of view, exclusive modes suffer from large hadronic uncertainties due to the form factors. One has to find strategies to reduce this form factor dependence by considering appropriate ratios. On the contrary, the experimental measurements are easier here compared to the case of inclusive modes.

Two kinematic regimes are considered in order to avoid the narrow $c\bar{c}$ resonances. In the region where the dimuon invariant mass squared q^2 is small ($1 < q^2 < 6\ \text{GeV}^2$), the decay is described by the QCD-improved factorization (QCDF) and the soft-collinear effective theory (SCET). In the high-q^2 region ($q^2 \gtrsim 14\ \text{GeV}^2$), on the other hand, the operator product expansion (OPE) is used. As the theoretical

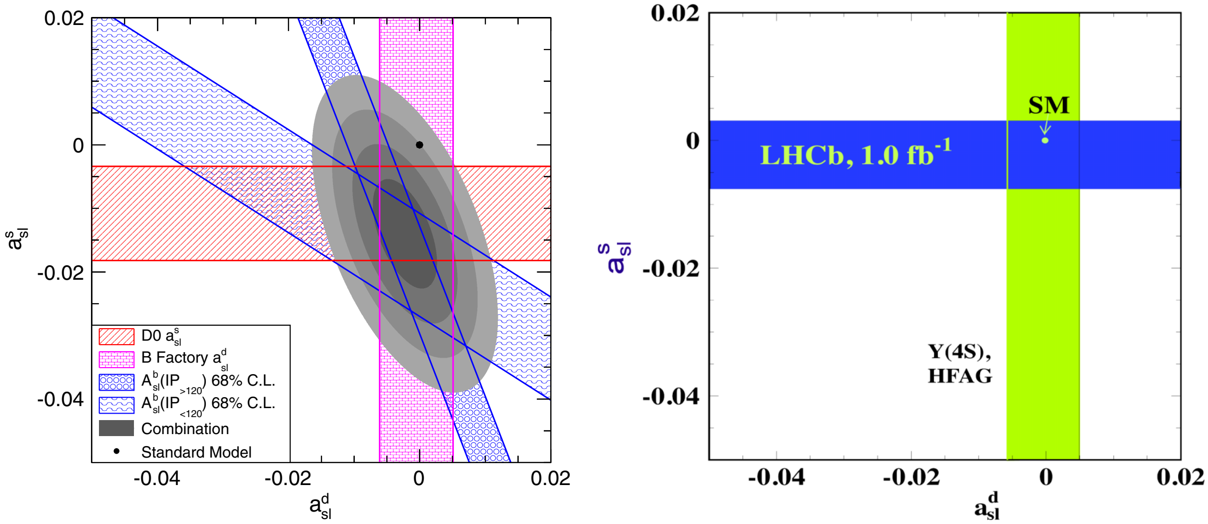

FIG. 9 (color online). Measurements of the semileptonic *CP* asymmetries a_{sl}^{d} and a_{sl}^{s} by D0 [left (Abazov *et al.*, 2013)] and by LHCb and *B* factories [right (LHCb Collaboration, 2012a)].

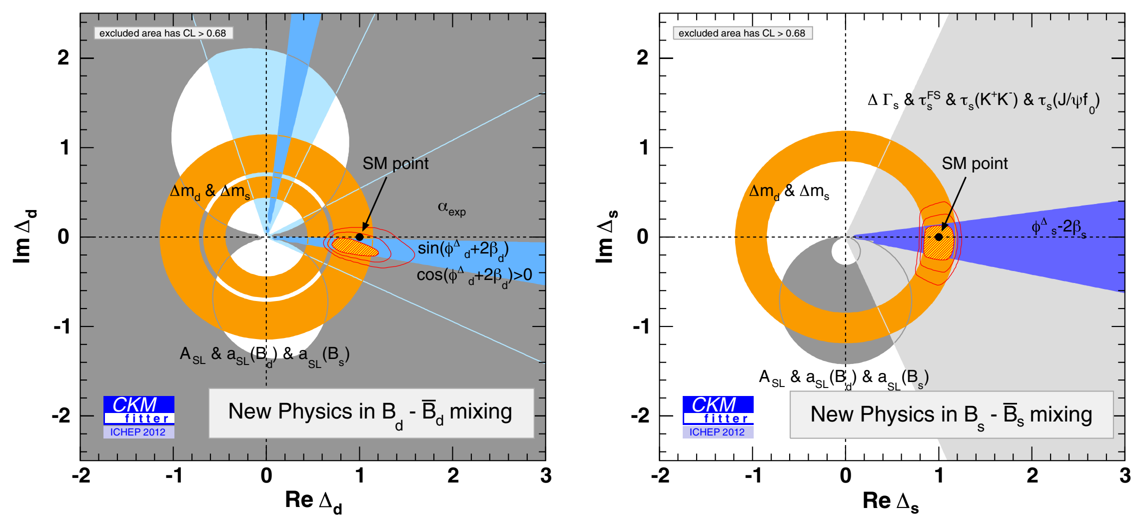

FIG. 10 (color online). New physics in B_d-$\bar{B}_d$ (left) and in B_s-$\bar{B}_s$ (right) mixing: fit result for the complex parameters Δ_d and Δ_s, respectively. The hashed area shows the region with <68.3% C.L. while the two additional contour lines inscribe the regions with <95.45% C.L. and <99.73% C.L., respectively. From Charles *et al.*, 2005.

treatments in the low- and high-q^2 regions are based on different concepts, the consistency of the consequences from the two regimes allows for important cross-checks.

The angular distribution of $B \to K^* \ell^+ \ell^-$ with $K^* \to K^+ \pi^-$ can be fully described in terms of four kinematic variables: the angles θ_ℓ, θ_K, ϕ, and q^2 as shown in Fig. 11. There are 12 angular terms appearing in the differential decay rate that can be exploited experimentally. The full expressions for these functions can be found in Egede *et al.* (2008, 2010).

Several angular observables, namely, the differential branching ratio, forward-backward asymmetry ($A_{\rm FB}$), and K^* longitudinal fraction (F_L), have already been measured by the Belle and *BABAR* experiments, and also CDF and LHCb. In addition, LHCb also measured S_3 which is related to the asymmetry between the K^* parallel and perpendicular spin amplitudes and the value of q_0^2 for which the differential forward-backward asymmetry vanishes. The experimental results as well as the SM predictions for these observables are summarized in Table I. They agree within the current errors.

In the constrained minimal supersymmetric standard model (CMSSM), $A_{\rm FB}$ and q_0^2 are particularly constraining. The CMSSM is governed by only five additional universal parameters defined at the $M_{\rm GUT}$ scale: the mass of the scalar particles m_0, the mass of the gauginos $m_{1/2}$, the trilinear coupling A_0, the ratio of the vacuum expectation values of the Higgs doublet $\tan\beta$, and finally the sign of the Higgsino mass term μ. In Fig. 12 the supersymmetric (SUSY) spread is compared to the LHCb 1σ and 2σ bounds in the CMSSM parameter space with $\tan\beta = 50$ and $A_0 = 0$ (Mahmoudi, Neshatpour, and Orloff, 2012).

With 2–3 fb^{-1} of integrated luminosity, LHCb will have the opportunity of performing a full angular analysis. This

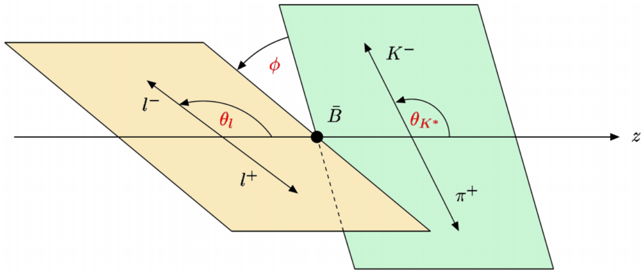

FIG. 11 (color online). Kinematic variables in $B \to K^* \ell^+ \ell^-$.

calls in turn for an optimized set of observables with reduced theoretical uncertainty. In particular, as the amplitudes depend linearly on the soft form factors at leading order in the low-q^2 region, a complete cancellation of the hadronic uncertainties could be possible in leading order, which consequently increases the sensitivity to new physics. In the high-q^2 region, there are improved Isgur-Wise relations between the form factors which allow one to construct optimal observables.

Examples of such observables are the transversity amplitudes $A_T^{(2,3,4,5)}$ (Egede *et al.*, 2008, 2010) [or similarly $P_{1\cdots6}$ (Matias *et al.*, 2012) and $H_T^{(1,2,3)}$ (Bobeth, Hiller, and van Dyk, 2010)]. The sensitivity of $A_T^{(2)}$ to NP scenarios is illustrated in Fig. 13. A large number of analyses exist on the NP sensitivity showing the rich phenomenology of the angular observables (Bobeth, Hiller, and Piranishvili, 2008; Egede *et al.*, 2008, 2010; Altmannshofer *et al.*, 2009; Bobeth, Hiller, and van Dyk, 2010, 2011; Beaujean *et al.*, 2012; Mahmoudi, Neshatpour, and Orloff, 2012; Matias *et al.*, 2012).

C. Implications of the latest measurements of $B_s \to \mu\mu$

The rare decay $B_s \to \mu^+\mu^-$ proceeds via Z^0 penguin and box diagrams in the SM; see Fig. 14. It is highly helicity suppressed by a suppression factor m_μ/m_b on the amplitude level. As a consequence the SM prediction for the branching ratio of the decay $B_s \to \mu^+\mu^-$ is of the order of 10^{-9}. However, the branching ratio can be much larger within specific extensions of the SM. For example, the helicity suppression of the SM contribution leads to an enhanced sensitivity to the Higgs-mediated scalar FCNCs within the two-Higgs doublet model (2HDM) and, especially within the MSSM; see Fig. 14. These nonstandard contributions lead to a drastic enhancement in the large $\tan\beta$ limit (Huang, Liao, and Yan, 1998; Hamzaoui, Pospelov, and Toharia, 1999; Babu and Kolda, 2000). In the MSSM there is an enhancement factor of $(\tan\beta)^3$ on the amplitude level. The best upper limit for $\mathrm{BR}(B_s \to \mu^+\mu^-)$ measured in a single experiment comes from LHCb (Aaij *et al.*, 2012c):

$$\mathrm{BR}(B_s \to \mu^+\mu^-) < 4.5 \times 10^{-9} \tag{13}$$

at 95% C.L. This upper limit is followed by the result from CMS, $\mathrm{BR}(B_s \to \mu^+\mu^-) < 7.7 \times 10^{-9}$ (Chatrchyan *et al.*, 2012b). The CDF Collaboration obtains a 95% C.L. upper limit $\mathrm{BR}(B_s \to \mu^+\mu^-) < 3.4 \times 10^{-8}$ (Aaltonen *et al.*, 2011), together with a 1σ interval $\mathrm{BR}(B_s \to \mu^+\mu^-) = (1.3^{+0.9}_{-0.7}) \times 10^{-8}$, coming from an observed excess over the expected background. The ATLAS Collaboration announced the upper limit $\mathrm{BR}(B_s \to \mu^+\mu^-) < 2.2 \times 10^{-8}$ (Aad *et al.*, 2012b). The combination of LHCb, ATLAS, and CMS results leads to an upper bound of 4.2×10^{-9} (LHCb/CMS/ATLAS Collaborations, 2012).

TABLE I. Post- and pre-LHCb results for rare decays with the updated SM predictions (Mahmoudi, 2009).

Observable	Experiment (post-LHCb)	Experiment (pre-LHCb)	SM prediction
$\mathrm{BR}(B_s \to \mu^+\mu^-)$	$(3.2^{+1.4+0.5}_{-1.2-0.3}) \times 10^{-9}$ (Aaij *et al.*, 2013)	$<5.8 \times 10^{-8}$ (Aaltonen *et al.*, 2008)	$(3.53 \pm 0.38) \times 10^{-9}$
$\langle d\mathrm{BR}/dq^2(B \to K^*\mu^+\mu^-)\rangle_{q^2\in[1,6]\ \mathrm{GeV}^2}$	$(0.42 \pm 0.04 \pm 0.04) \times 10^{-7}$ (LHCb Collaboration, 2012a)	$(0.32 \pm 0.11 \pm 0.03) \times 10^{-7}$ (CDF Collaboration, 2010)	$(0.47 \pm 0.27) \times 10^{-7}$
$\langle d\mathrm{BR}/dq^2(B \to K^*\mu^+\mu^-)\rangle_{q^2\in[14.18,16]\ \mathrm{GeV}^2}$	$(0.59 \pm 0.07 \pm 0.04) \times 10^{-7}$ (LHCb Collaboration, 2012a)	$(0.83 \pm 0.20 \pm 0.07) \times 10^{-7}$ (CDF Collaboration, 2010)	$(0.71 \pm 0.18) \times 10^{-7}$
$\langle A_{\mathrm{FB}}(B \to K^*\mu^+\mu^-)\rangle_{q^2\in[1,6]\ \mathrm{GeV}^2}$	$-0.18 \pm 0.06 \pm 0.02$ (LHCb Collaboration, 2012a)	$0.43 \pm 0.36 \pm 0.06$ (CDF Collaboration, 2010)	-0.06 ± 0.05
$\langle A_{\mathrm{FB}}(B \to K^*\mu^+\mu^-)\rangle_{q^2\in[14.18,16]\ \mathrm{GeV}^2}$	$0.49 \pm 0.06 \pm 0.05$ (LHCb Collaboration, 2012a)	$0.42 \pm 0.16 \pm 0.09$ (CDF Collaboration, 2010)	0.44 ± 0.10
$q_0^2(A_{\mathrm{FB}}(B \to K^*\mu^+\mu^-))$	$4.9^{+1.1}_{-1.3}$ GeV^2 (LHCb Collaboration, 2012a)	$\cdots$	4.26 ± 0.34 GeV^2
$\langle F_L(B \to K^*\mu^+\mu^-)\rangle_{q^2\in[1,6]\ \mathrm{GeV}^2}$	$0.66 \pm 0.06 \pm 0.04$ (LHCb Collaboration, 2012a)	$0.50 \pm 0.30 \pm 0.03$ (CDF Collaboration, 2010)	0.72 ± 0.13
$\mathrm{BR}(B \to X_s\gamma)$	$(3.43 \pm 0.21 \pm 0.07) \times 10^{-4}$ (Amhis *et al.*, 2012)	$(3.43 \pm 0.21 \pm 0.07) \times 10^{-4}$ (Amhis *et al.*, 2012)	$(3.08 \pm 0.24) \times 10^{-4}$
$\Delta_0(B \to K^*\gamma)$	$(5.2 \pm 2.6) \times 10^{-2}$ (Amhis *et al.*, 2012)	$(5.2 \pm 2.6) \times 10^{-2}$ (Amhis *et al.*, 2012)	$(8.0 \pm 3.9) \times 10^{-2}$
$\mathrm{BR}(B \to X_d\gamma)$	$(1.41 \pm 0.57) \times 10^{-5}$ (del Amo Sanchez *et al.*, 2010; Wang, 2011)	$(1.41 \pm 0.57) \times 10^{-5}$ (del Amo Sanchez *et al.*, 2010; Wang, 2011)	$(1.49 \pm 0.30) \times 10^{-5}$
$\mathrm{BR}(B \to X_s\mu^+\mu^-)_{q^2\in[1,6]\ \mathrm{GeV}^2}$	$(1.60 \pm 0.68) \times 10^{-6}$ (Aubert *et al.*, 2004; Iwasaki *et al.*, 2005)	$(1.60 \pm 0.68) \times 10^{-6}$ (Aubert *et al.*, 2004; Iwasaki *et al.*, 2005)	$(1.78 \pm 0.16) \times 10^{-6}$
$\mathrm{BR}(B \to X_s\mu^+\mu^-)_{q^2>14.4\ \mathrm{GeV}^2}$	$(4.18 \pm 1.35) \times 10^{-7}$ (Aubert *et al.*, 2004; Iwasaki *et al.*, 2005)	$(4.18 \pm 1.35) \times 10^{-7}$ (Aubert *et al.*, 2004; Iwasaki *et al.*, 2005)	$(2.19 \pm 0.44) \times 10^{-7}$

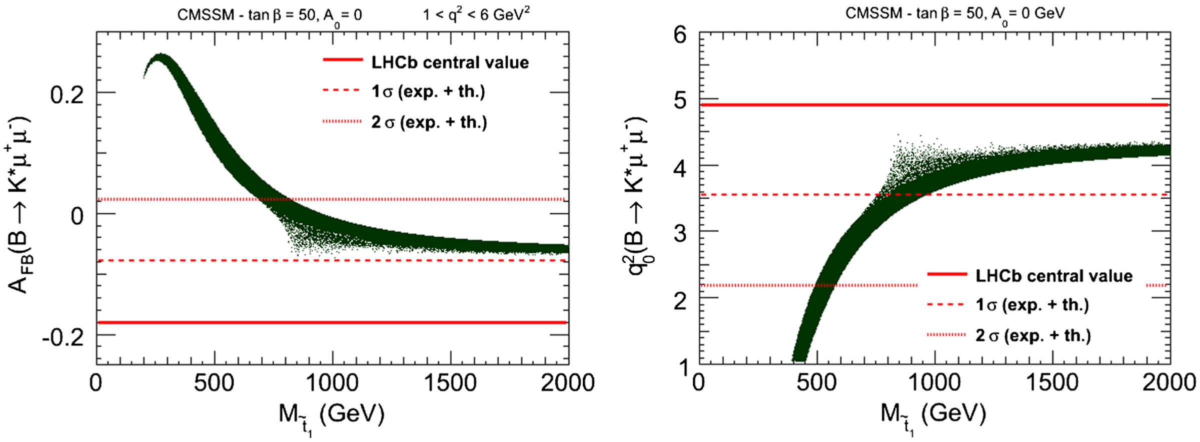

FIG. 12 (color online). SUSY spread of A_{FB} (left) and the A_{FB} zero crossing q_0^2 (right) as a function of the lightest stop mass in the CMSSM for $\tan\beta = 50$ and $A_0 = 0$.

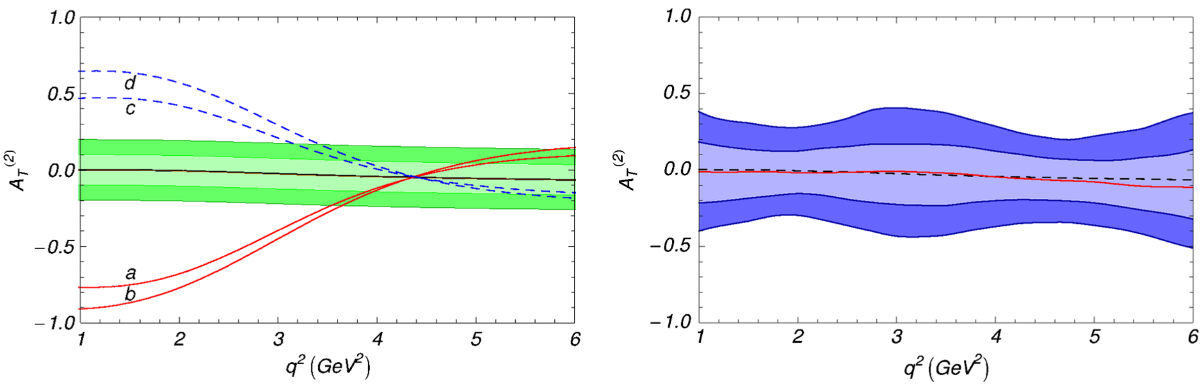

FIG. 13 (color online). The theoretical errors (left) for $A_T^{(2)}$ are compared to the experimental errors (right) as a function of q^2. Light bands include an estimated Λ/m_b uncertainty at a $\pm 5\%$ level and the dark bands correspond to a $\pm 10\%$ correction. The curves *(a)–(d)* correspond to different benchmark SUSY scenarios. In the right plot, the light and dark bands correspond to 1σ and 2σ statistical errors with a yield corresponding to 10 fb^{-1} data from LHCb, respectively. From Egede *et al.*, 2008.

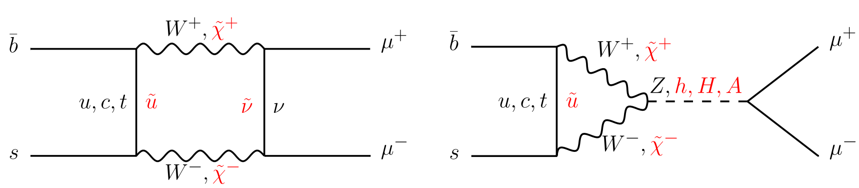

FIG. 14 (color online). Contributions to the rare decay $B_s \to \mu^+\mu^-$ in the SM (black) and in the MSSM (light).

Recently, the LHCb Collaboration announced the first evidence for the decay $\mathrm{BR}(B_s \to \mu^+\mu^-)$ with the branching ratio (Aaij *et al.*, 2013):

$$\mathrm{BR}(B_s \to \mu^+\mu^-) = [3.2^{+1.4}_{-1.2}(\mathrm{stat})^{+0.5}_{-0.3}(\mathrm{syst})] \times 10^{-9}. \tag{14}$$

This new measurement is a major step which will hopefully be followed by more precise results. The present accuracy, however, does not lead to improved constraints on supersymmetry as compared to the one from the previous upper limit. Nevertheless, as we will see, the lower bound has consequences on the constraints on the Wilson coefficients in the MFV framework.

All these results are very close to the SM prediction, which is $\mathrm{BR}(B_s \to \mu^+\mu^-) = (3.53 \pm 0.38) \times 10^{-9}$ (Mahmoudi, Neshatpour, and Orloff, 2012). The main theoretical uncertainty comes from the B_s decay constant, which is now in the focus of the lattice gauge theory community; see Davies (2011), Neil *et al.* (2011), Bazavov *et al.* (2012), Dimopoulos *et al.* (2012), McNeile *et al.* (2012), and Na *et al.* (2012).

The theoretical prediction does not directly correspond to the experimental branching ratio. There are two correction factors of $O(10\%)$: one includes the effect of the $\bar{B}_s$-B_s oscillation (De Bruyn *et al.*, 2012a, 2012b), and the other takes into account effects of soft radiation (Buras *et al.*, 2012).

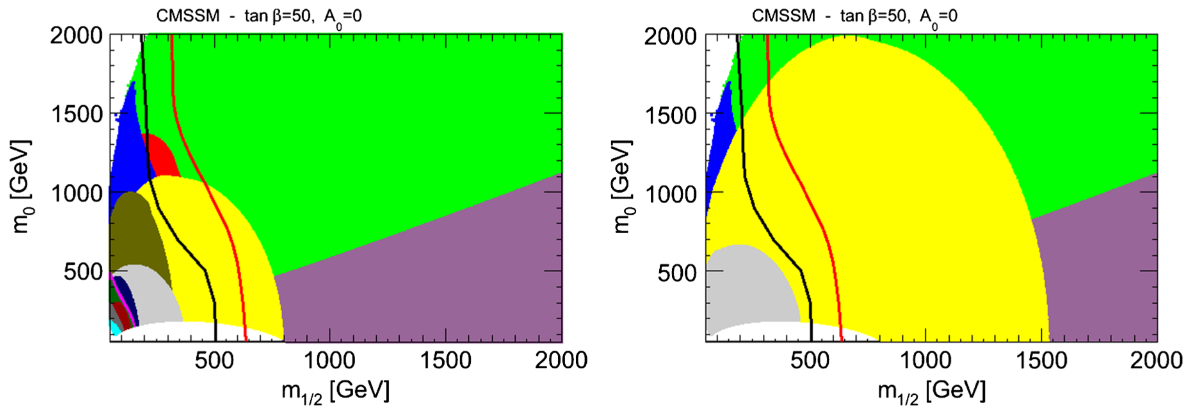

FIG. 15 (color online). Constraints from flavor observables on the CMSSM in the plane $(m_{1/2}, m_0)$ for $\tan\beta = 50$ with 2010 results on $\mathrm{BR}(B_s \to \mu^+\mu^-)$ (left) and with the 2011 results (right).

In an exemplary mode we show the strong restriction power of these data on the parameter space of the CMSSM as presented by Akeroyd, Mahmoudi, and Santos (2011) and Mahmoudi (2012). In Fig. 15, from Mahmoudi (2012), constraints from flavor observables on the CMSSM in the plane $(m_{1/2}, m_0)$ for a typical large $\tan\beta$ scenario with $\tan\beta = 50$ and $A_0 = 0$ are shown on the left with the 2011 results for $\mathrm{BR}(B_s \to \mu^+\mu^-)$, and on the right with the 2012 Moriond results. The color code is as in Fig. 16. The left vertical line corresponds to the CMS SUSY exclusion limit with 1.1 fb^{-1} of data (Chatrchyan *et al.*, 2011) and the right vertical line corresponds to the CMS SUSY exclusion limit with 4.4 fb^{-1} of data (CMS Collaboration (2012) at 7 TeV. One notes that while with more integrated luminosity the direct limit is slightly shifted to higher masses, the constraining power of the new $\mathrm{BR}(B_s \to \mu^+\mu^-)$ limit has impressively increased and overpassed the direct limit for high values of $\tan\beta$.

Figure 16 shows that while the rare decay $\mathrm{BR}(B_s \to \mu^+\mu^-)$ is very constraining in the large $\tan\beta$ region, it loses sensitivity when considering smaller values for $\tan\beta$. This conclusion does not change when considering more general MSSM scenarios with no universality assumption imposed. The sensitivity of the $B_s \to \mu^+\mu^-$ rate is significant in specific regions of the SUSY parameter space, mostly at large values of $\tan\beta$. As a result, as shown in Arbey *et al.* (2012), the current LHCb measurement, and even foreseen future improvements in its accuracy, leave a major fraction of the SUSY parameter space, compatible with the results of direct searches, unconstrained. However, if a SUSY particle is discovered in direct searches at ATLAS and CMS, the precise value of $\mathrm{BR}(B_s \to \mu^+\mu^-)$ would be very important for consistency checks and could be used to severely constrain the parameters and help discriminating between different hypotheses.

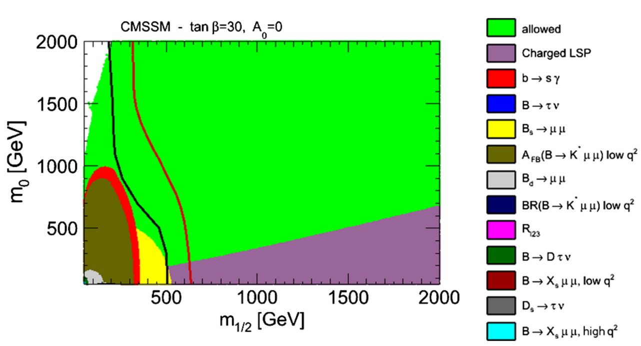

FIG. 16 (color online). Constraints from flavor observables in CMSSM in the plane $(m_{1/2}, m_0)$ for $\tan\beta = 30$.

III. LATEST NEWS FROM THE B FACTORIES

A. News on inclusive penguins?

The inclusive decay $\bar{B} \to X_s\gamma$ is a good example to confirm the simple CKM theory of flavor mixing in the SM, not shown in the CKM unitarity fit. While nonperturbative corrections to this decay mode are subleading and recently estimated to be well below 10% (Benzke *et al.*, 2010), perturbative QCD corrections are the most important corrections. Within a global effort, a perturbative QCD calculation to the next-to-next-to-leading-logarithmic (NNLL) order level has been performed and has led to the first NNLL prediction of the $\bar{B} \to X_s\gamma$ branching fraction (Misiak *et al.*, 2007) with a photon cut at $E_\gamma = 1.6$ GeV (including the error due to nonperturbative corrections):

$$\mathrm{BR}(\bar{B} \to X_s\gamma)_{\mathrm{NNLL}} = (3.15 \pm 0.23) \times 10^{-4}. \quad (15)$$

Using updated input parameters from the Particle Data Group (PDG), in particular, for the quark masses and the CKM elements, the central value is shifted to 3.08×10^{-4}. The combined experimental data by the Heavy Flavor Average Group (HFAG) leads to (Amhis *et al.*, 2012)

$$\mathrm{BR}(\bar{B} \to X_s\gamma) = (3.43 \pm 0.21 \pm 0.07) \times 10^{-4}, \quad (16)$$

where the first error is combined statistical and systematic, and the second is due to the extrapolation in the photon energy. Thus, the SM prediction and the experimental average are consistent at the 1.2σ level. As a consequence, the $\bar{B} \to X_s\gamma$ has very restrictive power on the parameter space of NP models. Recently, the first practically complete NLL calculation of this decay in the MSSM has been finalized (Greub, Hurth, Pilipp, and Schuepbach, 2011; Greub, Hurth, Pilipp, Schupbach, and Steinhauser, 2011).

The inclusive semileptonic decay $B \to X_s\ell^+\ell^-$ could in principle play a similar role in the NP search. The NNLL

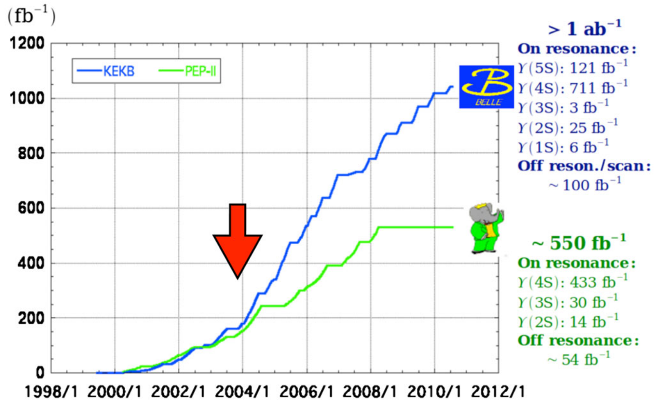

FIG. 17 (color online). Integrated luminosity of the B factories.

QCD calculation was finalized some time ago and even electromagnetic corrections have been calculated recently. The theoretical accuracy is of the order of 10% (Huber, Hurth, and Lunghi, 2008). However, unfortunately the *latest* measurements of this inclusive decay mode of the B factories stem from 2004 in the case of *BABAR* based on $89 \times 10^6 B\bar{B}$ events (Aubert *et al.*, 2004) and from 2005 in the case of Belle based on $152 \times 10^6 B\bar{B}$ events (Iwasaki *et al.*, 2005). The graph of the integrated luminosity (see Fig. 17) shows these numbers of events correspond to less than 30% of the data set available at the end of the B factories. It would be highly desirable that new analyses are worked out which are based on the complete data sets. For further details on inclusive penguin decays we refer the interested reader to the recent minireview on penguins (Hurth, 2012).

B. New physics in $B \to \tau\nu$?

For some time there has been tension between the direct measurement and the indirect fit of the branching ratio $\mathrm{BR}(B \to \tau\nu)$ at the 2.8σ level. Moreover, as pointed out by the CKM fitter group (Charles *et al.*, 2005), there has been a specific correlation between $\sin\beta$ and $\mathrm{BR}(B \to \tau\nu)$ which is also a bit at odds; see Fig. 18. Obviously the measured value of $\sin\beta$ has been too low, while the one of $\mathrm{BR}(B \to \tau\nu)$ has been too large. Interestingly, this tension could have been solved by a negative NP mixing phase in the B_d system $\Phi_d^{\Delta} < 0$.

In principle, one could think that this tension could also be solved by a NP contribution to $\mathrm{BR}(B \to \tau\nu)$ induced by a charged Higgs in the popular 2HDM of type II; see the left diagram in Fig. 19. In the later model the SM branching ratio gets modified in the following way:

$$\mathrm{BR}(B \to \tau\nu) = \mathrm{BR}_{\mathrm{SM}} \times \left(1 - \frac{m_B^2}{M_{H^+}^2}\tan^2\beta\right)^2. \qquad (17)$$

But for the allowed values of the ratio of the quantity $\tan\beta$ and the charged Higgs mass M_{H^+} due to constraints by other flavor data one only gets a reduction compared to the SM branching ratio.

However, Belle recently presented a new measurement with new data and an improved analysis method also including a reanalysis of the old data which shows a significant lower value in good agreement with the global fit, while the new *BABAR* measurement confirms the old high value. The various measurements are shown in Fig. 20. As a result

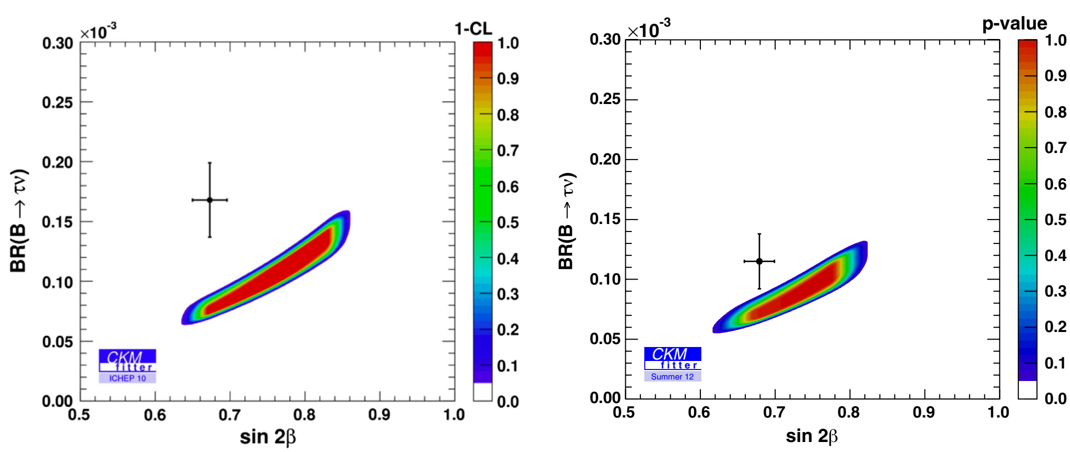

FIG. 18 (color online). Correlation of $\mathrm{BR}(B \to \tau\nu)$ and $\sin\beta$ based on pre-ICHEP12 data (left) and on ICHEP12 data (right); the cross corresponds to the experimental values with 1σ uncertainties. From Charles *et al.*, 2005.

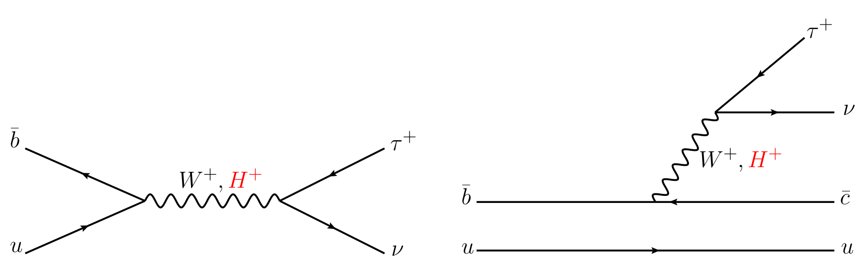

FIG. 19 (color online). Tree contributions to $\mathrm{BR}(B \to \tau\nu)$ (left) and to $\mathrm{BR}(B \to D\tau\nu)$ (right).

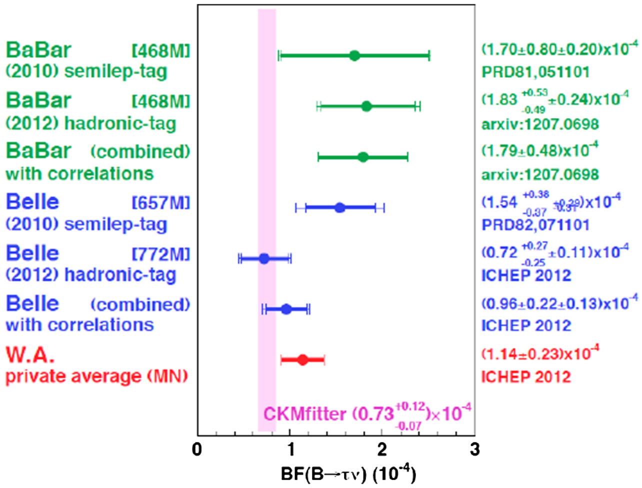

FIG. 20 (color online). ICHEP12 data: various measurements of $\mathrm{BR}(B \to \tau\nu)$ with the new world average. Courtesy of M. Nakao.

the indirect fit prediction for $\mathrm{BR}(B \to \tau\nu)$ and direct measurements presently deviate by 1.6σ only; see Fig. 18.

Recently a similar tension showed up in $B \to D\tau\nu$ and $B \to D^*\tau\nu$. Based on its full data sample, *BABAR* reported improved measurements of the specific ratios (Lees *et al.*, 2012):

$$\mathcal{R}_{\tau/\ell} = \mathrm{BR}(B \to D\tau\nu)/\mathrm{BR}(B \to D\ell\nu) = 0.440 \pm 0.058 \pm 0.018, \tag{18}$$

$$\mathcal{R}^*_{\tau/\ell} = \mathrm{BR}(B \to D^*\tau\nu)/\mathrm{BR}(B \to D^*\ell\nu) = 0.332 \pm 0.024 \pm 0.018. \tag{19}$$

They exceed the SM expectations by 2.0σ and 2.7σ, respectively (Bailey *et al.*, 2012; Becirevic, Kosnik, and Tayduganov, 2012; Fajfer, Kamenik, and Nisandzic, 2012; Fajfer, Kamenik, Nisandzic, and Zupan, 2012).

These ratios are rather sensitive to new physics contributions because the hadronic form factors tend to cancel. For example, they are sensitive to the charged Higgs; see the right diagram in Fig. 19. But again the 2HDM-II does not offer a consistent explanation of the two ratios; for the allowed values of $\tan\beta/M_{H^+}$, one finds an explanation for $\mathcal{R}$ but not for $\mathcal{R}^*$. As shown in Crivellin, Greub, and Kokulu (2012), a consistent explanation of both ratios is possible in the 2HDM of type III. Interestingly, Fajfer, Kamenik, and Nisandzic (2012) and Fajfer, Kamenik, Nisandzic, and Zupan (2012) argued that minimal flavor violation (MFV) (see next section) is disfavored as an explanation of this anomaly and spot various models with general flavor structures for it. Since the current result still suffers from large systematic uncertainty due to the background, the updated *BABAR* results and confirmation from Belle are awaited to clarify the situation.

IV. MFV BENCHMARK

At this stage of the NP search using rare B and kaon decays, it makes sense to analyze the impact of the measurements within the framework of MFV. The hypothesis of MFV (Chivukula and Georgi, 1987; Hall and Randall, 1990; D'Ambrosio *et al.*, 2002; Hurth *et al.*, 2009) is a formal model-independent solution to the NP flavor problem. It assumes that the flavor and the CP symmetries are broken as in the SM. Thus, it requires that all flavor- and CP-violating interactions be linked to the known structure of Yukawa couplings. A renormalization-group invariant definition of MFV based on a symmetry principle is given by D'Ambrosio *et al.* (2002); this is mandatory for a consistent effective field theoretical analysis of NP effects [for a recent minireview, see Isidori and Straub (2012)].

The MFV hypothesis represents an important benchmark in the sense that any measurement which is inconsistent with the general constraints and relations induced by the MFV hypothesis unambiguously indicates the existence of new flavor structures. Moreover, compared with a general model-independent analysis as presented by Descotes-Genon *et al.* (2011), Altmannshofer and Straub (2012), and Beaujean *et al.* (2012), the number of free parameters is heavily reduced due to the additional MFV relations. Indeed there are two strict predictions in this general class of models which have to be tested. First the MFV hypothesis implies the usual CKM relations between $b \to s$, $b \to d$, and $s \to d$ transitions. For example, this relation allows for upper bounds on NP effects in $\mathrm{BR}(\bar{B} \to X_d\gamma)$ and $\mathrm{BR}(\bar{B} \to X_s\nu\bar{\nu})$ using experimental data or bounds from $\mathrm{BR}(\bar{B} \to X_s\gamma)$ and $\mathrm{BR}(K \to \pi^+\nu\bar{\nu})$, respectively. This emphasizes the need for high-precision measurements of $b \to s/d$, but also of $s \to d$ transitions such as the rare kaon decay $K \to \pi\nu\bar{\nu}$. The second prediction is that the CKM phase is the only source of CP violation. This implies that any phase measurement as in $B \to \phi K_s$ is not sensitive to new physics. This is an additional assumption because the breakings of the flavor group and the discrete CP symmetry are in principle not connected at all. For example, there is also a renormalization-group invariant extension of the MFV concept allowing for flavor-blind phases as shown by Hurth, Lunghi, and Porod (2005); however, these lead to nontrivial CP effects, which get strongly constrained by flavor-diagonal observables such as electric dipole moments (Hurth, Lunghi, and Porod, 2005). So within the model-independent effective field theory approach of MFV we keep the minimality condition regarding CP. But in specific models like MSSM the discussion of additional CP phases within the MFV framework makes sense and can also allow for a natural solution of the well-known supersymmetric CP problem; see, for example, Mercolli and Smith (2009) and Paradisi and Straub (2010).

The application of the MFV hypothesis to the MSSM offers two attractive features. First, most interestingly, the MFV hypothesis can serve as a substitute for R parity in the MSSM (Nikolidakis and Smith, 2008; Csaki, Grossman, and Heidenreich, 2012). MFV is sufficient to forbid a too fast proton decay because when the MFV hypothesis is applied to R-parity violating terms, the spurion expansion leads to a suppression by neutrino masses and light-charged fermion masses. In this sense MFV within the MSSM can be regarded as a natural theory for R-parity violation. Second, the MFV framework is renormalization-group invariant by construction; however, it is not clear that the hierarchy between the spurion terms is preserved when running down from the high scale to the low electroweak scale. Without this conservation of hierarchy, the MFV hypothesis would lose its practicability. However, as shown by Paradisi, Ratz, and Schieren (2008) and Colangelo, Nikolidakis, and Smith (2009), a MFV-compatible change of the boundary conditions at the high scale has barely any influence on the low-scale spectrum.

It is worth mentioning that the MFV hypothesis solves the NP flavor problem only formally. One still has to find explicit dynamical structures to realize the MFV hypothesis such as gauge-mediated supersymmetric theories. And of course the MFV hypothesis is not a theory of flavor; it does not explain the hierarchical structure of the CKM matrix and the large mass splittings of the SM fermions.

We stress that the MFV hypothesis is far from being verified. There is still room for sizable new effects, and new flavor structures beyond the Yukawa couplings are still compatible with the present data because the flavor sector has been tested only at the 10% level especially in the $b \to s$ transitions.

Based on the recent LHCb data a new analysis of rare decays within the MFV effective theory was presented (Hurth and Mahmoudi, 2012). Here we update that analysis using the latest LHCb result for $\mathrm{BR}(B_s \to \mu^+\mu^-)$ and the new HFAG world average for $\mathrm{BR}(B \to X_s\gamma)$.

Within the MFV effective Hamiltonian one singles out only five relevant $b \to s$ operators (and also $b \to d$ operators with obvious replacements):

$$\begin{aligned}
\mathcal{H}_{\rm eff}^{b\to s} = &-\frac{4G_F}{\sqrt{2}}[V_{us}^* V_{ub}(C_1^c P_1^u + C_2^c P_2^u) \\
&+ V_{cs}^* V_{cb}(C_1^c P_1^c + C_2^c P_2^c)] \\
&-\frac{4G_F}{\sqrt{2}}\sum_{i=3}^{10}[(V_{us}^* V_{ub} + V_{cs}^* V_{cb})C_i^c \\
&+ V_{ts}^* V_{tb} C_i^t]P_i + V_{ts}^* V_{tb} C_0^\ell P_0^\ell + \text{H.c.},
\end{aligned} \tag{20}$$

where the relevant operators are

$$\begin{aligned}
P_7 &= \frac{e}{16\pi^2} m_b(\bar{s}_L \sigma^{\mu\nu} b_R) F_{\mu\nu}, \\
P_8 &= \frac{g_s}{16\pi^2} m_b(\bar{s}_L \sigma^{\mu\nu} T^a b_R) G^a_{\mu\nu}, \\
P_9 &= \frac{e^2}{16\pi^2}(\bar{s}_L \gamma_\mu b_L)\sum_\ell(\bar{\ell}\gamma^\mu \ell), \\
P_{10} &= \frac{e^2}{16\pi^2}(\bar{s}_L \gamma_\mu b_L)\sum_\ell(\bar{\ell}\gamma^\mu \gamma_5 \ell), \\
P_0^\ell &= \frac{e^2}{16\pi^2}(\bar{s}_L b_R)(\bar{\ell}_R \ell_L).
\end{aligned} \tag{21}$$

The NP contributions to the corresponding Wilson coefficients can be parametrized as

$$\delta C_i = C_i^{\rm MFV} - C_i^{\rm SM}. \tag{22}$$

We scan over δC_7, δC_8, δC_9, δC_{10}, and δC_0^ℓ in order to obtain constraints on the Wilson coefficients based on the experimental results. Consecutively, for each point, the flavor observables are computed with the SUPERISO program (Mahmoudi, 2008, 2009). The obtained values are compared to the experimental results by calculating the χ^2 in the usual way and the global fits are obtained by minimization of the χ^2.

The individual constraints from the new $\mathrm{BR}(\bar{B} \to X_s\gamma)$ and $\mathrm{BR}(B_s \to \mu^+\mu^-)$ results are displayed in Fig. 21. Compared to the previous constraints in Hurth and Mahmoudi (2012), the region favored by $\mathrm{BR}(\bar{B} \to X_s\gamma)$ is only slightly shifted, and the constraints from the upper bound of $\mathrm{BR}(B_s \to \mu^+\mu^-)$ weakened while the lower bound now excludes the central region.

Two global MFV fits are given in Fig. 22 to make the significance of the latest LHCb data manifest. In the first row, the experimental data before the start of the LHCb experiment are used (pre-LHCb), while the plots in the second row include the latest LHCb measurements (post-LHCb), as given in Table I. Here C_8 is mostly constrained by $\bar{B} \to X_{s,d}\gamma$, while C_7 is constrained by many other observables as well. C_9 is highly affected by $b \to s\mu^+\mu^-$ (inclusive and exclusive). C_{10} is in addition further constrained by $B_s \to \mu^+\mu^-$. The coefficient C_0^ℓ of the scalar operator is dominantly constrained by $B_s \to \mu^+\mu^-$. There are always two allowed regions at 95% C.L. in the correlation plots within the post-LHCb fit: one corresponds to SM-like MFV coefficients and one to coefficients with flipped sign. The allowed region with the SM is more favored. The various δC_i correlation plots show the flipped sign for C_7 is possible only if C_9 and C_{10} receive large nonstandard contributions which finally also change the sign of these coefficients. With the help of the results of the global fit, which restricts the NP contributions δC_i, we can now derive several interesting predictions for observables which are not yet well measured. This analysis also allows one to spot the observables which still allow for relatively large deviations from the SM (even in the MFV benchmark scenario). The following MFV predictions at the 95% C.L. are of particular interest:

$$1.0\times 10^{-5} < \mathrm{BR}(\bar{B} \to X_d\gamma) < 4.0\times 10^{-5}, \tag{23}$$

$$\mathrm{BR}(B_d \to \mu^+\mu^-) < 3.8\times 10^{-10}. \tag{24}$$

The present experimental results are (del Amo Sanchez *et al.*, 2010; Wang, 2011; Aaij *et al.*, 2013)

$$\mathrm{BR}(\bar{B} \to X_d\gamma)_{\rm Exp} = (1.41 \pm 0.57)\times 10^{-5}, \tag{25}$$

$$\mathrm{BR}(B_d \to \mu^+\mu^-)_{\rm Exp} < 9.4\times 10^{-10}. \tag{26}$$

So the present $\bar{B} \to X_d\gamma$ measurement is already below the MFV bound and is nicely consistent with the correlation between the decays $\bar{B} \to X_s\gamma$ and $\bar{B} \to X_d\gamma$ predicted in the MFV scenario. In the case of the leptonic decay $B_d \to \mu^+\mu^-$, however, the MFV bound is stronger than the current experimental limit. Moreover, there are still sizable deviations from the SM prediction possible within and also beyond the MFV bound but an enhancement by orders of magnitude (i.e., due to large $\tan\beta$ effects) is already ruled out by the latest measurements. Clearly, a measurement of $B_d \to \mu^+\mu^-$ beyond the MFV bound would signal the existence of new flavor structures beyond the Yukawa couplings.

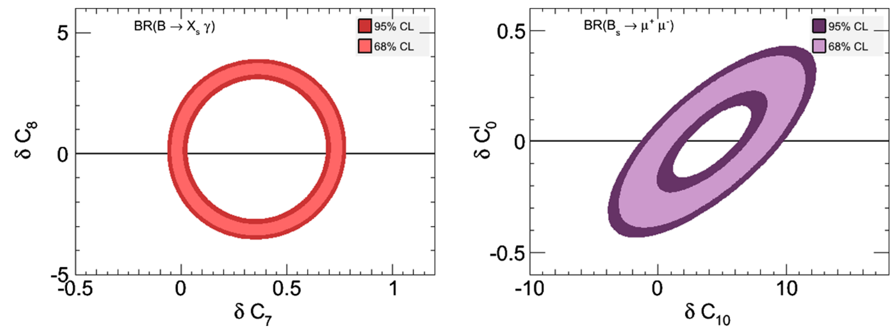

FIG. 21 (color online). 68% and 95% C.L. bounds on δC_7 and δC_8 induced by the inclusive decay $\bar{B} \to X_s \gamma$ (left) and on δC_{10} and δC_0^ℓ induced by the decay $B_s \to \mu^+ \mu^-$ (right).

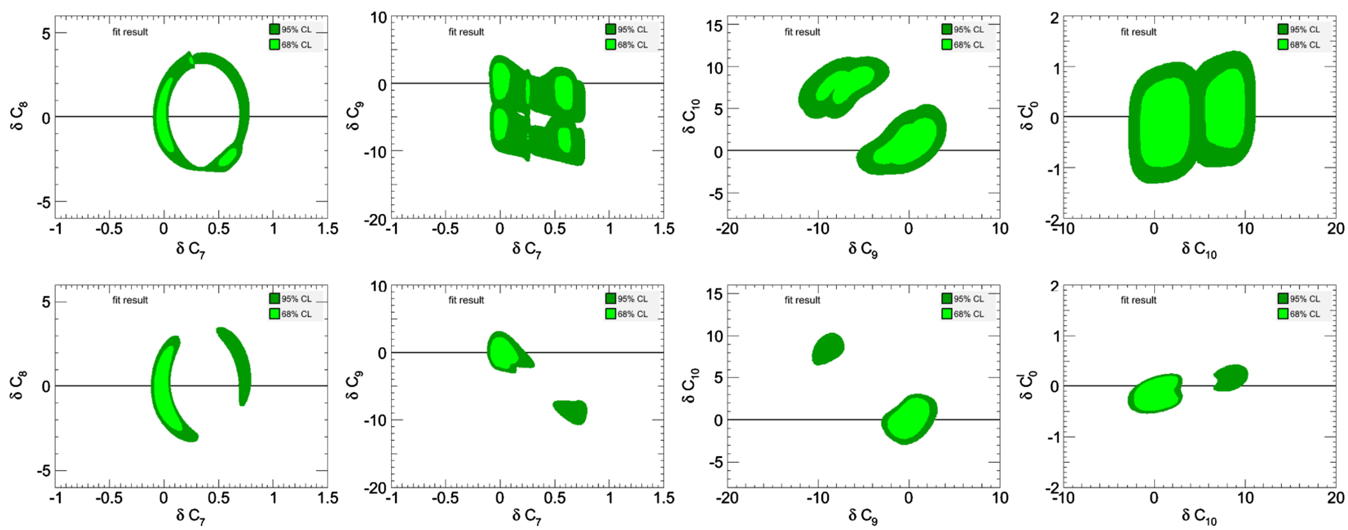

FIG. 22 (color online). Global MFV fit to the various NP coefficients δC_i in the MFV effective theory *without* (upper panel) and *with* experimental data of LHCb (lower panel).

V. OUTLOOK AND FUTURE OPPORTUNITIES

Many efforts have been deployed in the past in order to calculate as precisely as possible the low energy observables from flavor physics. This global effort led to a very satisfying situation now as we have access to several observables for which the theoretical predictions have reached high levels of accuracy. The reliability of the results from flavor physics (as compared to the other indirect searches such as in the dark matter sector where strong astrophysical and cosmological assumptions are needed) makes the flavor observables the premier actors in the search for indirect NP effects. Rare B decays and, in particular, $b \to s\gamma$ are the main assets here. Also the fact that multiple observables are available offers the opportunity for important cross-checks.

In addition, any discovery at a high-p_T experiment must be consistent with the measurement from flavor experiments—the contrary would indicate an inconsistency in the theory. The role of flavor physics is therefore very important in the LHC era.

An example of the interplay between flavor constraints and LHC direct search results is displayed in Fig. 23 for the 2HDM type II, where BR($b \to s\gamma$) excludes the charged Higgs mass below 345 GeV for any value of $\tan\beta$. BR($B \to \tau\nu$), on the other hand, more strongly constrains larger values of $\tan\beta$. These constraints can be compared to the latest limit from the direct searches of the charged Higgs boson by ATLAS (Aad *et al.*, 2012a) (dashed line), where flavor constraints are clearly stronger, or with the CMS limit from direct $H/A \to \tau^+\tau^-$ searches (Chatrchyan *et al.*,

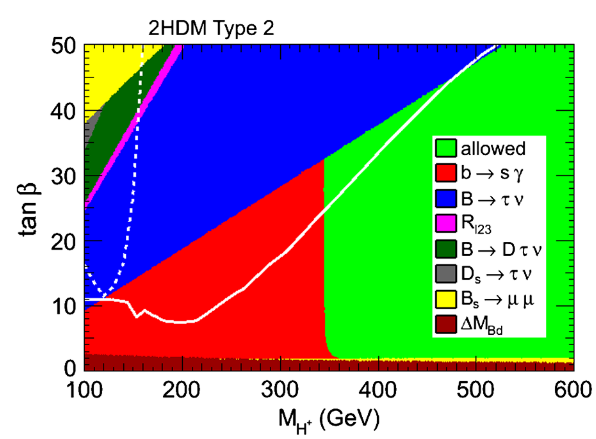

FIG. 23 (color online). Constraints from flavor observables in the 2HDM type II in the plane (M_{H^+}, $\tan\beta$). The right area corresponds to the parameter space still allowed by the flavor constraints. The constraints of the direct searches are indicated by the dashed or solid line (see text).

2012a) (solid line); here the CMS limit on M_A has been transformed into a limit on M_{H^+} assuming the tree-level MSSM mass relation $M_{H^+}^2 = M_A^2 + M_W^2$. One notices the consistency and complementarity of the direct and indirect results. Another concrete example is the understanding of the newly discovered Higgs-like particle properties where imposing consistency with the $b \to s\gamma$ and $B_s \to \mu^+\mu^-$ results allows one to discriminate between some of the underlying hypotheses.

We know that the stabilization of the electroweak sector needs a nontrivial flavor structure which still has to be clearly identified. In spite of the fact that the first two years of high-statistics measurements of LHCb have not found any NP in FCNCs, still sizable deviations from the MFV scenario are possible in various flavor observables. Thus, higher precision is needed to separate small deviations from the MFV benchmark.

Also in other future scenarios for particle physics, flavor physics will be important. For example, in case no NP is discovered next to one scalar Higgs particle, the flavor precision experiments may show us the way to the NP energy scale. FCNCs provide indirect information about scales which are not accessible by the direct search.

There are great experimental opportunities in flavor physics in the near future which will push the experimental precision to its limit. There are B physics programs at LHC at all three experiments at CERN. Especially LHCb will collect 5 times more data than the present data set. The copious production of all flavors of B mesons at the LHC, together with the unique particle-identification capabilities of the LHCb detector, makes it possible to investigate a wide range of decay channels that have not been accessible to previous experiments. Most of them have been discussed in this Colloquium such as the CP-violating phase β_s, and searches of new physics effects via the rare decay modes $B \to K^*\mu\mu$ and $B_s \to \mu\mu$, but also the measurement of the unitarity angle γ and $B_s \to \phi\phi$. An upgrade of the LHCb experiment with a final integrated luminosity of 5 to 50 fb^{-1} is planned and already approved (Merk, 2011).

There are also forthcoming experiments measuring rare K decays such as $K^+ \to \pi^+\nu\bar{\nu}$ and $K_L \to \pi^0\nu\bar{\nu}$ (JPARC Kaon Collaboration; NA48 Collaboration) which are extremely sensitive to possible new degrees of freedom and are largely unexplored.

In addition, two super-B factories, Belle II at KEK (Abe, 2010; Aushev *et al.*, 2010) and SuperB in Italy (Bona *et al.*, 2007; Hitlin *et al.*, 2008; O'Leary *et al.*, 2010), have been approved and partially funded to accumulate 2 orders of magnitude larger data samples.[1] The super-B factories are actually *super-flavor* factories (SFF): Besides precise B measurements[for example, the present experimental error of BR($B \to \tau\nu$) discussed above will be reduced from 20% down to 4% improving the NP reach of this observable significantly]the SFF allow for precise analyses of CP violation in charm and of lepton flavor-violating modes like $\tau \to \mu\gamma$ [see Browder *et al.* (2008)]. The results will be highly complementary to those on several important observables related to B_s meson oscillations, kaon, and muon decays that will be measured elsewhere.

Most important are the opportunities of a SFF for lepton flavor physics. The sensitivity for τ physics is far superior to any other existing or proposed experiment, and the physics reach can be extended even farther by the possibility to operate with polarized beams. The study of the correlation of neutrino properties with flavor phenomena in the charged-lepton and in the quark sector, e.g., charged-lepton flavor violation, is also an important target. Pushing the present limits on $\mu \leftrightarrow e$ and $\mu \leftrightarrow \tau$ transitions can lead to important insight. The combined information on μ and τ flavor-violating decays that will be provided by the MEG experiment (MEG Collaboration) together with a SFF (Browder *et al.*, 2008) may shed light on the mechanism responsible for lepton flavor violation.

[1]The Italian government has recently decided that the latest cost estimate of the project is not compatible with the budget of the National Plan for Research.

ACKNOWLEDGMENTS

T. H. thanks the CERN theory group for its hospitality during his regular visits to CERN where part of this work was written.

REFERENCES

Aad, G., *et al.* (ATLAS Collaboration), 2012a, J. High Energy Phys. 06, 039.

Aad, G., *et al.* (ATLAS Collaboration), 2012b, Phys. Lett. B **713**, 387.

Aaij, R., *et al.* (LHCb Collaboration), 2012a, Phys. Rev. Lett. **108**, 241801.

Aaij, R., *et al.* (LHCb Collaboration), 2012b, Phys. Rev. Lett. **108**, 101803.

Aaij, R., *et al.* (LHCb Collaboration), 2012c, Phys. Rev. Lett. **108**, 231801.

Aaij, R.,*et al.* (LHCb Collaboration), 2013, Phys. Rev. Lett. **110**, 021801.

Aaltonen, T., *et al.* (CDF Collaboration), 2008, Phys. Rev. Lett. **100**, 101802.

Aaltonen, T., *et al.* (CDF Collaboration), 2011, Phys. Rev. Lett. **107**, 191801.

Abazov, V., *et al.* (D0 Collaboration), 2013, Phys. Rev. Lett. **110**, 011801.

Abazov, V. M., *et al.* (D0 Collaboration), 2011, Phys. Rev. D **84**, 052007.

Abe, T., *et al.* (Belle II Collaboration), 2010, arXiv:1011.0352.

Akeroyd, A., F. Mahmoudi, and D. M. Santos, 2011, J. High Energy Phys. 12, 088.

Ali, A., and D. London, 1995, Z. Phys. C **65**, 431.

Altmannshofer, W., and D. M. Straub 2012, J. High Energy Phys. 08, 121.

Altmannshofer, W., *et al.*, 2009, J. High Energy Phys. 01, 019.

Amhis, Y., *et al.* (Heavy Flavor Averaging Group), 2012, arXiv:1207.1158.

Arbey, A., M. Battaglia, F. Mahmoudi, and D. M. Santos, 2012, arXiv:1212.4887.

ATLAS Collaboration, http://atlas.web.cern.ch.

Aubert, B., *et al.* (*BABAR* Collaboration), 2004, Phys. Rev. Lett. **93**, 081802.

Aushev, T., *et al.*, 2010, arXiv:1002.5012.

BABAR Collaboration, 1998, Report No. SLAC-R-0504.

BABAR Collaboration, http://www.slac.stanford.edu/BFROOT.

Babu, K., and C. F. Kolda, 2000, Phys. Rev. Lett. **84**, 228.
Bailey, J. A., *et al.*, 2012, Phys. Rev. Lett. **109**, 071802.
Bazavov, A., *et al.* (Fermilab Lattice Collaboration, MILC Collaboration), 2012, Phys. Rev. D **85**, 114506.
Beaujean, F., C. Bobeth, D. van Dyk, and C. Wacker, 2012, J. High Energy Phys. 08, 030.
Becirevic, D., N. Kosnik, and A. Tayduganov, 2012, Phys. Lett. B **716**, 208.
Belle Collaboration, http://belle.kek.jp.
Benzke, M., S. J. Lee, M. Neubert, and G. Paz, 2010, J. High Energy Phys. 08, 099.
Bobeth, C., G. Hiller, and G. Piranishvili, 2008, J. High Energy Phys. 07, 106.
Bobeth, C., G. Hiller, and D. van Dyk, 2010, J. High Energy Phys. 07, 098.
Bobeth, C., G. Hiller, and D. van Dyk, 2011, J. High Energy Phys. 07, 067.
Bona, M., *et al.* (SuperB Collaboration), 2007, arXiv:0709.0451.
Browder, T., *et al.*, 2008, J. High Energy Phys. 02, 110.
Buras, A. J., J. Girrbach, D. Guadagnoli, and G. Isidori, 2012, Eur. Phys. J. C **72**, 2172.
Cabibbo, N., 1963, Phys. Rev. Lett. **10**, 531.
CDF Collaboration, 2010, Report No. CDF-note-10047.
CDF Collaboration, http://www-cdf.fnal.gov/physics/new/bottom/bottom.html.
Charles, J., *et al.* (CKMfitter Group), 2005, Eur. Phys. J. C **41**, 1, and updated results and plots available at http://ckmfitter.in2p3.fr, arXiv:hep-ph/0406184.
Chatrchyan, S., *et al.* (CMS Collaboration), 2011, Phys. Rev. Lett. **107**, 221804.
Chatrchyan, S., *et al.* (CMS Collaboration), 2012a, Phys. Lett. B **713**, 68.
Chatrchyan, S., *et al.* (CMS Collaboration), 2012b, Phys. Rev. D **86**, 072010.
Chivukula, R. S., and H. Georgi, 1987, Phys. Lett. B **188**, 99.
CMS Collaboration, 2012, Report No. CMS-PAS-SUS-12-005.
CMS Collaboration, http://cms.web.cern.ch.
Colangelo, G., E. Nikolidakis, and C. Smith, 2009, Eur. Phys. J. C **59**, 75.
Crivellin, A., C. Greub, and A. Kokulu, 2012, Phys. Rev. D **86**, 054014.
Csaki, C., Y. Grossman, and B. Heidenreich, 2012, Phys. Rev. D **85**, 095009.
D0 Collaboration, http://www-d0.fnal.gov/Run2Physics/WWW/results/b.htm.
D'Ambrosio, G., G. Giudice, G. Isidori, and A. Strumia, 2002, Nucl. Phys. **B645**, 155.
Davies, C., 2011, Proc. Sci., LATTICE2011 019.
De Bruyn, K., *et al.*, 2012a, Phys. Rev. D **86**, 014027.
De Bruyn, K., *et al.*, 2012b, Phys. Rev. Lett. **109**, 041801.
del Amo Sanchez, P., *et al.* (*BABAR* Collaboration), 2010, Phys. Rev. D **82**, 051101.
Descotes-Genon, S., D. Ghosh, J. Matias, and M. Ramon, 2011, J. High Energy Phys. 06, 099.
Dimopoulos, P., *et al.* (ETM Collaboration), 2012, J. High Energy Phys. 01, 046.
Egede, U., T. Hurth, J. Matias, M. Ramon, and W. Reece, 2008, J. High Energy Phys. 11, 032.
Egede, U., T. Hurth, J. Matias, M. Ramon, and W. Reece, 2010, J. High Energy Phys. 10, 056.
Fajfer, S., J. F. Kamenik, and I. Nisandzic, 2012, Phys. Rev. D **85**, 094025.
Fajfer, S., J. F. Kamenik, I. Nisandzic, and J. Zupan, 2012, Phys. Rev. Lett. **109**, 161801.
Froggatt, C., and H. B. Nielsen, 1979, Nucl. Phys. **B147**, 277.
Gherghetta, T., and A. Pomarol, 2000, Nucl. Phys. **B586**, 141.
Greub, C., T. Hurth, V. Pilipp, and C. Schuepbach, 2011, arXiv:1111.3692.
Greub, C., T. Hurth, V. Pilipp, C. Schuepbach, and M. Steinhauser, 2011, Nucl. Phys. **B853**, 240.
Grossman, Y., and M. Neubert, 2000, Phys. Lett. B **474**, 361.
Hall, L., and L. Randall, 1990, Phys. Rev. Lett. **65**, 2939.
Hamzaoui, C., M. Pospelov, and M. Toharia, 1999, Phys. Rev. D **59**, 095005.
Hitlin, D., *et al.*, 2008, arXiv:0810.1312.
Huang, C.-S., W. Liao, and Q.-S. Yan, 1998, Phys. Rev. D **59**, 011701(R).
Huber, T., T. Hurth, and E. Lunghi, 2008, Nucl. Phys. **B802**, 40.
Hurth, T., 2003, Rev. Mod. Phys. **75**, 1159.
Hurth, T., 2012, AIP Conf. Proc. **1441**, 678.
Hurth, T., G. Isidori, J. F. Kamenik, and F. Mescia, 2009, Nucl. Phys. **B808**, 326.
Hurth, T., and S. Kraml, 2012, AIP Conf. Proc. **1441**, 713.
Hurth, T., E. Lunghi, and W. Porod, 2005, Nucl. Phys. **B704**, 56.
Hurth, T., and F. Mahmoudi, 2012, Nucl. Phys. **B865**, 461.
Hurth, T., and M. Nakao, 2010, Annu. Rev. Nucl. Part. Sci., **60**, 645.
Isidori, G., and D. M. Straub, 2012, Eur. Phys. J. C **72**, 2103.
Iwasaki, M., *et al.* (Belle Collaboration), 2005, Phys. Rev. D **72**, 092005.
JPARC Kaon Collaboration, http://kaon.kek.jp/~kpwg.
Kobayashi, M., and T. Maskawa, 1973, Prog. Theor. Phys. **49**, 652.
Lees, J., *et al.* (*BABAR* Collaboration), 2012, Phys. Rev. Lett. **109**, 101802.
Lenz, A., 2011, arXiv:1108.1218.
Lenz, A., and U. Nierste, 2011, arXiv:1102.4274.
Lenz, A., *et al.*, 2011, Phys. Rev. D **83**, 036004.
Lenz, A., *et al.*, 2012, Phys. Rev. D **86**, 033008.
LHCb/CMS/ATLAS Collaborations, 2012, Report Nos. LHCb-CONF-2012-017, CMS-PAS-BPH-12-009, ATLAS-COM-CONF-2012-090.
LHCb Collaboration, 2012a, Report No. LHCb-CONF-2012-008.
LHCb Collaboration, 2012b, Report No. LHCb-CONF-2012-022.
LHCb Collaboration, http://lhcb.web.cern.ch/lhcb/.
Mahmoudi, F., 2008, Comput. Phys. Commun. **178**, 745.
Mahmoudi, F., 2009, Comput. Phys. Commun. **180**, 1579.
Mahmoudi, F., 2012, arXiv:1205.3099.
Mahmoudi, F., S. Neshatpour, and J. Orloff, 2012, J. High Energy Phys. 08, 092.
Matias, J., F. Mescia, M. Ramon, and J. Virto, 2012, J. High Energy Phys. 04, 104.
McNeile, C., C. Davies, E. Follana, K. Hornbostel, and G. Lepage, 2012, Phys. Rev. D **85**, 031503.
MEG Collaboration, http://meg.web.psi.ch.
Mercolli, L., and C. Smith, 2009, Nucl. Phys. **B817**, 1.
Merk, M., *et al.* (LHCb Collaboration) 2011, Proc. Sci., BEAUTY2011 039.
Misiak, M., *et al.*, 2007, Phys. Rev. Lett. **98**, 022002.
NA48 Collaboration, http://na48.web.cern.ch/NA48/NA48-3.
Na, H., *et al.*, 2012, Phys. Rev. D **86**, 034506.
Neil, E., *et al.* (Fermilab Lattice Collaboration, MILC Collaboration), 2011, Proc. Sci., LATTICE2011, 320.
Nelson, A. E., and M. J. Strassler 2000, J. High Energy Phys. 09, 030.
Nikolidakis, E., and C. Smith, 2008, Phys. Rev. D **77**, 015021.
O'Leary, B., *et al.* (SuperB Collaboration), 2010, arXiv:1008.1541.
Paradisi, P., M. Ratz, R. Schieren, and C. Simonetto, 2008, Phys. Lett. B **668**, 202.
Paradisi, P., and D. M. Straub, 2010, Phys. Lett. B **684**, 147.
Randall, L., and R. Sundrum, 1999, Phys. Rev. Lett. **83**, 3370.
Wang, W., 2011, arXiv:1102.1925.